

Excitonic condensation in a symmetric electron-hole bilayer

S. De Palo,^{1,*} F. Rapisarda,^{2,†} and Gaetano Senatore^{1,3,‡}

¹*INFM - Istituto Nazionale di Fisica della Materia - Unità di Trieste*

²*Institut für Theoretische Physik, Johannes Kepler Universität, Altenberger Strasse 69, A-0404 Linz, Austria*

³*Dipartimento di Fisica Teorica, Università di Trieste, Strada Costiera 11, 34014 Trieste, Italy*

(Dated: 23 January, 2002)

Using Diffusion Monte Carlo simulations we have investigated the ground state of a symmetric electron-hole bilayer and determined its phase diagram at $T = 0$. We find clear evidence of an excitonic condensate, whose stability however is affected by in-layer electronic correlation. This stabilizes the electron-hole plasma at large values of the density or inter-layer distance, and the Wigner crystal at low density and large distance. We have also estimated pair correlation functions and low order density matrices, to give a microscopic characterization of correlations, as well as to try and estimate the condensate fraction.

PACS numbers: 71.35.-y, 71.10.-w, 73.21.-b

Electron-hole systems have attracted a lot of interest over the years [1]. The Coulomb attraction existing between the two kinds of Fermions naturally brings about pairing, and hence the possibility of a coherent state [2]. It was soon realized [3] that systems of spatially separated electrons and holes, such as a bilayer, have a number of advantages with respect to conventional bulk samples [1] in which electrons and holes occupy the same region. Thus, while in a homogeneous semiconductor the excitonic condensate would be an insulator [2], in a bilayer superconductivity is in principle possible [3]. The interest in such systems has greatly increased in recent years, due to the increasing ability to manufacture high quality semiconductor quantum well (QW) structures, where electrons and holes are indeed confined in different regions, between which tunneling can be made negligible [4]. Also, in a number of such systems experimental evidence of an excitonic condensate has been claimed [5, 6, 7]. However, even for the simplest two dimensional (2D) model, i.e., a symmetric bilayer, the theory has been concerned so far with mean-field treatments [3, 8, 9] based on a BCS like wavefunction, with one exception [10].

In this Letter we report on the first extensive computer simulations of a symmetric electron-hole bilayer (SEHB). We have undertaken this study to assess the effect of electron correlation on the phase diagram of the SEHB and on the existence of a condensate, which we directly characterize. To perform simulations, we have resorted to fixed-node diffusion Monte Carlo (FN-DMC) [11, 12], a method which is stable and variational and is known to yield extremely accurate results for homogeneous electron systems [13, 14]. We should stress that our goal is to determine the properties of the simplest 2D model, i.e., the SEHB, with unprecedented accuracy, also to provide a benchmark against which approximate many-body treatments may be tested. Therefore, we are not considering here effects such as finite layer thickness, inter-layer tunneling, or band anisotropy, which may play an im-

portant role [3, 15, 16] in describing more realistic QW structures. Also, to limit the computational load, we have restricted our study to three phases: the excitonic phase (EP), the spin unpolarized two component plasma (2CP), and the triangular Wigner crystal (WC).

In the absence of magnetic fields, the Hamiltonian of such an ideal SEHB reads

$$H_{eh} = - \sum_i \frac{\nabla_{i,e}^2}{2m_e} - \sum_i \frac{\nabla_{i,h}^2}{2m_h} + \sum_{i < j} \frac{e^2}{\epsilon |\mathbf{r}_{i,e} - \mathbf{r}_{j,e}|} + \sum_{i < j} \frac{e^2}{\epsilon |\mathbf{r}_{i,h} - \mathbf{r}_{j,h}|} - \sum_{i,j} \frac{e^2}{\epsilon \sqrt{|\mathbf{r}_{i,e} - \mathbf{r}_{j,h}|^2 + d^2}}, \quad (1)$$

with ϵ the background dielectric constant, d the inter-layer distance, and $m_e = m_h = m^*$ the common effective mass of electrons and holes. In the following we use $Ry^* = e^2/2\epsilon a_B^*$ as unit energy, $a_B^* = \hbar^2 \epsilon / m^* e^2$, and $r_s a_B^*$ as unit length. As is well known the parameter r_s , defined in terms of the in-layer areal density n by $\pi r_s^2 a_B^{*2} = 1/n$, measures the in-layer coupling strength. In the SEHB one is lead to define an additional parameter, measuring the importance of the inter-layer coupling, as the ratio of the typical inter-layer and in-layer Coulomb energies, namely $\gamma = 1/d$. At $T = 0$, which is the case considered here, the model is completely specified by r_s and d or γ .

In FN-DMC [11] one propagates a trial wavefunction Ψ_T in imaginary time, to project out the higher energy components and sample the lowest energy state Ψ_0 with the nodal structure of Ψ_T . This establishes a correspondence between nodal structure, i.e., trial function, and phase. To study the EP we resort to a BCS-like trial function, which is known to provide a good mean-field description [2, 9, 17] both at high and at low density. In practice we set $\Psi_T^{EP} = D_{\uparrow\uparrow} D_{\downarrow\downarrow} J$, where $D_{\sigma\sigma}$ is a determinant of pair orbitals $\varphi(\mathbf{r}_{i,\sigma}^e - \mathbf{r}_{j,\sigma}^h)$ and J is a Jastrow factor, accounting for two-body correlations. We choose $\varphi(r)$ as the exact numerical solution of the mean-field problem [9], as in selected cases we found that this yields a lower variational energy than other choices [18].

TABLE I: Energy per particle of various phases of the SEHB, in Ry^* , according to FN-DMC. All results are extrapolated to the thermodynamic limit [23].

r_s	d	r_E	2CP	E	WC
1	0.0	1.69	-0.833(8)	-0.808(9)	
2	0.1	0.84	-0.6947(5)	-0.6976(7)	
2	0.2	1.00	-0.6116(7)	-0.6006(7)	
2	0.5	1.34	-0.5405(5)	-0.5260(4)	
5	0.2	0.57	-0.3732(6)	-0.3822(2)	
5	0.5	0.93	-0.3125(2)	-0.3104(1)	
5	1.0	1.40	-0.3009(2)	-0.2987(2)	
10	0.5	0.68	-0.1801(1)	-0.18172(9)	
10	1.0	1.23	-0.17153(8)	-0.17085(4)	
10	1.5		-0.17035(1)		-0.16947(1)
20	0.05	0.14	-0.3275(2)	-0.3288(1)	
20	0.5	0.50	-0.10051(5)	-0.10227(3)	-0.10157(2)
20	1.0	1.08	-0.09304(1)	-0.09316(2)	-0.093176(8)
20	1.3	1.38	-0.09264(2)	-0.09261(2)	
20	1.5	1.51	-0.09260(2)	-0.09248(2)	-0.092533(5)
20	3.0		-0.09245(2)		-0.092354(6)
22	1.0		-0.08533(2)		-0.085484(7)
22	2.0		-0.08482(1)		-0.084770(6)
22	3.0		-0.08478(1)		-0.084767(5)
30	0.5	0.45		-0.07192(2)	-0.07161(2)
30	1.0	1.00		-0.064403(8)	-0.064483(3)
30	1.5	1.48		-0.063833(6)	-0.063921(3)
30	3.0			-0.06377(7)	-0.063827(3)

For the normal phases the trial function is taken as $\Psi_T = D_{\downarrow}^e D_{\uparrow}^e D_{\downarrow}^h D_{\uparrow}^h J$, with D_{σ}^a a Slater determinant of one-particle orbitals (plane waves for the 2CP and gaussians localized at the crystal sites[19] for the WC). The Jastrow factor $J = \exp[-(1/2) \sum_{\mu,\nu} \sum'_{i_{\mu},i_{\nu}} u_{\mu,\nu}(r_{i_{\mu},i_{\nu}})]$, with the Greek index denoting particle type and spin projection, is built using RPA pseudopotentials [20, 21].

We have performed DMC simulations for systems with $N = 58$ and $N = 56$ particles per layer, respectively for the 2CP and the EP and for the WC, using periodic boundary conditions. Finite size effects have been mitigated as usual [22] by performing the Ewald summation on the infinite periodic replicas of the simulation *box* and using, for the 2CP, numbers of particles corresponding to closed shells of orbitals. We have also carried out variational Monte Carlo (VMC) simulations, for several values of N (ranging up to 114 or 120 depending on the phase), to determine the size dependence [23] of the energy. Assuming that this is the same for VMC and FN-DMC [13, 24, 25], we have obtained the FN-DMC energies in the thermodynamic limit, which we report [26] in Table I for the three phases that we have studied.

Use of the energies of Table I yields the phase dia-

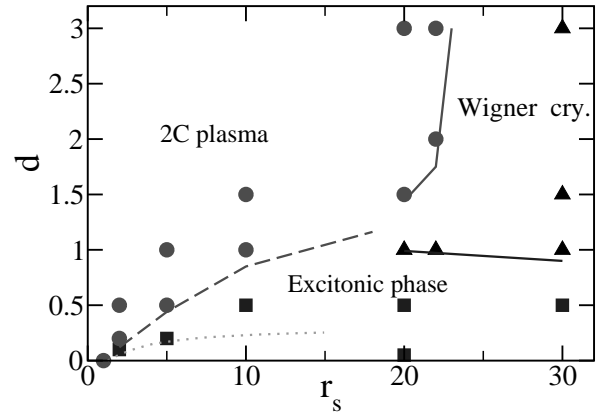


FIG. 1: Phase diagram of the SEHB according to the FN-DMC. Circles, squares and triangles respectively indicate the stability of the 2CP, EP, and WC. Dashed, gray and black lines give approximate boundaries between pair of phases obtained from the crossing of the energies at given r_s with varying d . The dotted curve reports an estimate of the 2CP-EP boundary from an approximate theory [30].

gram shown in Fig. 1. It is evident that correlation has here qualitative effects. Whereas the mean-field predicts stability of the EP with respect to the 2CP everywhere, at high enough density and/or at large enough distance FN-DMC predicts the stability of either the 2CP or the WC. Naively, one would expect that when the inter-layer coupling $\gamma = 1/d \ll 1$ each layer should behave as an isolated 2D electron gas (2DEG) [27]. This is the case with the symmetric electron bilayer [20, 28, 29], for which the phase diagram of the 2DEG [28] is quickly recovered as d exceeds 1, and it appears to be the case also for the SEHB, when one keeps in mind that only the unpolarized 2CP is considered here. The phase diagram turns out to be fairly robust. Thus, use of the finite- N FN-DMC energies leaves it essentially unchanged, while use of the VMC energies only brings about a minor change in the boundary between the WC and the 2CP, which moves at about $r_s = 20$ for $d \geq 1.5$.

In Table I we have also reported the excitonic radius, defined by $r_E^2 = \langle \varphi | r^2 | \varphi \rangle / \langle \varphi | \varphi \rangle$. It is evident, from an inspection of the Table, that a correlation exists between the stability of the EP and r_E being smaller than 1, i.e., smaller than the characteristic in-layer length scale. This points to the importance of in-layer correlations, which are neglected in mean-field [3, 9]. Also, it turns out that in our simulations the *exciton* is always much smaller than the side of the simulation *box*, $\sqrt{N}\pi \simeq 13$. Thus, our description of the EP should not be affected by the finite spacing of the energy levels [10].

A peculiar property of superconductors is the off-diagonal long-range order (ODLRO) exhibited by the reduced density matrices in the coordinate space representation [31]. In a Fermion system ODLRO shows up in

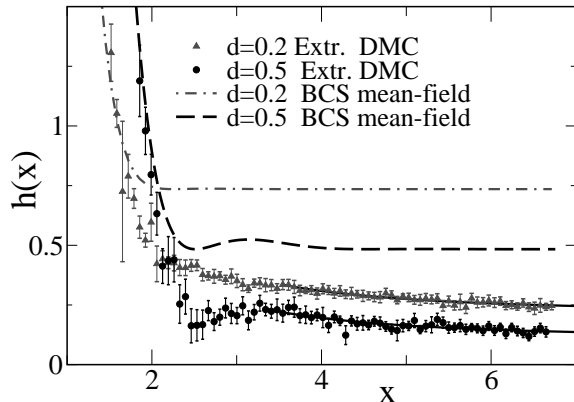


FIG. 2: Projected two-body density matrix of the SEHB at $r_s = 5$, according to FN-DMC and BCS mean-field, for $N = 58$. The full curves are fits to the tails of the simulation data (see text and Table II for details).

TABLE II: Condensate fraction α of the SEHB according to FN-DMC (extrapolated estimate) and VMC, for a system with $N=58$. Here $\tilde{d} = d \cdot r_s$ is the interlayer distance in units of a_B^* . Also reported are the BCS mean-field prediction and, for FN-DMC, the reduced χ^2 of the fit yielding the condensate fraction (see text).

r_s	\tilde{d}	$\alpha(\text{BCS})$	$\alpha(\text{VMC})$	$\alpha(\text{FN-DMC})$	χ^2
2	0.2	0.55	0.187(4)	0.284(9)	0.59
5	1.0	0.74	0.151(2)	0.215(4)	0.22
5	2.5	0.48	0.095(3)	0.108(5)	0.34
20	1.0	0.98	0.027(1)	0.020(2)	0.47

the two-body density matrix [31], with the appearance of an eigenvalue which scales with the number of particles. In a translational invariant system, such as the SEHB in the excitonic phase, ODLRO implies for the two-body density matrix, to leading order in N , the following asymptotic behavior:

$$\rho_2(\mathbf{x}'_e, \mathbf{x}'_h; \mathbf{x}_e, \mathbf{x}_h) = \alpha N f^*(|\mathbf{x}'_e - \mathbf{x}'_h|) f(|\mathbf{x}_e - \mathbf{x}_h|), \quad (2)$$

$$|\mathbf{x}_e - \mathbf{x}_h|, |\mathbf{x}'_e - \mathbf{x}'_h| \lesssim \xi, \quad |\mathbf{x}_e - \mathbf{x}'_e| \rightarrow \infty,$$

where $\alpha \leq 1$ is the condensate fraction and ξ is the range of the normalized pair amplitude $f(|\mathbf{x}_1 - \mathbf{x}_2|)$. In order to estimate the condensate fraction it is convenient to resort to the projected two-body density matrix (P2BDM)

$$h(x) = \frac{1}{N} \int d\mathbf{x}_e d\mathbf{x}_h \rho_2(\mathbf{x}_e + \mathbf{x}, \mathbf{x}_h + \mathbf{x}; \mathbf{x}_e, \mathbf{x}_h), \quad (3)$$

which tends to α in the large x limit, as is immediately found combining Eqs. (2) and (3).

A simple estimator of $h(x)$ is given by

$$h(x) = \frac{N}{M_c} \sum_{i=1}^{M_c} \frac{\Psi_T(\mathbf{R}'_i)}{\Psi_T(\mathbf{R}_i)}, \quad (4)$$

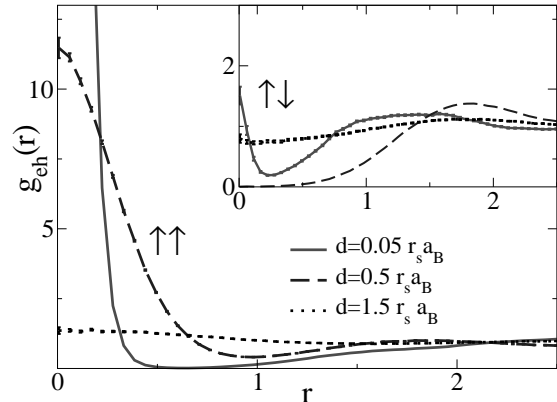


FIG. 3: Spin resolved electron-hole pair correlation function of the SEHB at $r_s = 20$, according to FN-DMC.

with M_c the number of particle configurations used and \mathbf{R}' obtained from the configuration \mathbf{R} by rigidly translating an electron-hole pair [32] by \mathbf{x} . In practice, for each \mathbf{R} we generate a few translations \mathbf{x} uniformly distributed in the simulation *box* and, for better statistics, we also average Eq. (4) over all electron-hole pairs. As Eq. (4) only yields a mixed estimate in DMC, we have also performed VMC calculations to get extrapolated estimates [34] according to $h_{Ext}(x) = 2h_{DMC}(x) - h_{VMC}(x)$.

An illustration of our results for $h(x)$ is given in Fig. 2. Indeed, $h(x)$ appears to saturate at large x . In the absence of exact information on its asymptotic form, we have fitted its tail to $\alpha + A/x^2$, $x \geq 5$ and estimated the condensate fractions reported in Table II for the cases studied. It is evident that in-layer correlation, which is absent in mean field, causes a substantial reduction of the condensate fraction—a reduction which becomes more pronounced with increasing the in-layer coupling r_s , at given interlayer distance, and to less extent with increasing the interlayer distance, at given r_s . This effect is particularly strong at large coupling, yielding the essential suppression of the condensate at $r_s = 20$ and $d = 0.05$, with $\alpha \simeq 0.02$ whereas in mean field $\alpha \simeq 1$.

Additional insight into the nature of the phases of the SEHB is provided by the pair correlation functions, whose features we briefly summarize here. As the two layers are brought together from infinity inter-layer interaction produces a substantial buildup in inter-layer correlations and the screening and weakening of intra-layer correlations, as for the electron bilayer [20, 28, 29]. However, while $g_{eh}(r)$ and $g_{eh}^{\uparrow\uparrow}(r)$ monotonously increase with decreasing d , near the origin, $g_{eh}^{\uparrow\downarrow}(r)$, first develops a *correlation hole* and then by further diminishing d develops a peak. This behavior, which becomes particularly marked at large coupling as is evident from Fig. 3, might be interpreted as a tendency toward biexciton formation for large r_s and small d . In fact, $g_{eh}^{\uparrow\downarrow}(r)$ gives correlations

between unpaired ($\uparrow\downarrow$) electrons and holes and, indirectly, between \uparrow and \downarrow excitons.

To summarize, by performing extensive quantum simulations we have shown that correlation has important qualitative effects in determining the phase diagram and the excitonic condensate of the SEHB, with respect to mean-field. Here, we have chosen not to consider spin polarized phases nor inhomogeneities of spin or charge, such as in density waves and in liquid-vapor coexistence. We shall explore some of these interesting phenomena in future investigations.

We acknowledge useful discussions with many colleagues and among the others with D. Neilson, C. Castellani, R.K. Moudgil. SDP and GS respectively acknowledge the holding of INFM fellowships while carrying out this work and support by MURST through COFIN99.

* Present address: INFM -Istituto Nazionale di Fisica della Materia - Unità di Roma

† Present address: Product and Business Development Group, Banca IMI, Milano, Italy

‡ senatore@ts.infn.it

- [1] T.M.Rice, *Solid State Phys.* **32**, 1 (1977); J.C.Hensel, T.G Phillips, and G.A. Thomas, *ibid.* **32**, 88 (1977).
- [2] L.V. Keldish and Y.V. Kopaev, *Fiz. Tverd. Tela* **6** 2791 (1964) [*Sov. Phys. Solid State* **6**, 2219 (1965)]; A.N.Kozlov and L.A. Maximov, *Zh. Eksp. Teor. Fiz.* **48**, 1184 (1965)[*Sov. Phys. JEPT* **21**, 790 (1965)]; L.V. Keldish and A.N.Kozlov, *Zh. Eksp. Teor. Fiz.* **54**, 1978 (1968)[*Sov. Phys. JEPT* **27**, 521 (1968)].
- [3] Yu. E. Lozovik and V. I. Yudson, *Pis'ma Zh. Eksp. Teor. Fiz.* **22**, 556 (1975)[*JETP Lett.* **22**, 274 (1975)]; *Solid State Commun.* **19**, 391 (1976); *Zh. Eksp. Teor. Fiz.* **71**, 738 (1976) [*Sov. Phys. JETP* **44**, 389 (1976)].
- [4] U.Sivan, P.M. Solomon and H. Shtrikman, *Phys. Rev. Lett* **68**, 1196 (1992); B. Kane *et al.*, *Appl. Phys. Lett.* **65**, 3266 (1994).
- [5] L.V. Butov *et al.* *Phys. Rev. Lett.* **73**, 304 (1994).
- [6] V.B. Timofeev *et al.* *Phys. Rev.* **B 61**, 8420 (2000).
- [7] J. P Cheng *et al.*, *Phys. Rev. Lett.* **74**, 450 (1995) J. Kono *et al.*, *Phys. Rev.* **B 55**, 1617 (1997); T.P. Marlow *et al.*, *Phys. Rev. Lett.* **82**, 2362 (1999).
- [8] Y.E. Lozovik and O.L. Berman, *Physica Scrip.* **55**, 491 (1997).
- [9] Xuejun Zhu, P.B. Littlewood, S. Hybersten and T. M. Rice, *Phys. Rev. Lett* **74**, 1633 (1995), P.B. Littlewood and Xuejun Zhu, *Phys. Scripta* **T 68**, 56 (1996).
- [10] Antony Chan, PhD Thesis, Indiana University (1996).
- [11] P. J. Reynolds, D. M. Ceperley, B. J. Alder and W.A. Lester, *J. Chem. Phys.* **77**, 5593 (1982); see also C. J. Umrigar, M.P. Nightingale and K.J Runge, *J. Chem. Phys.* **99**, 2865 (1993).
- [12] For a recent survey of QMC methods see, e.g., *Quantum Monte Carlo Methods in Physics and Chemistry*, ed. M.P. Nightingale and C.J. Umrigar (Kluwer, Dordrecht, 1999).
- [13] Y. Kwon, D.M Ceperley, and R.M. Martin, *Phys. Rev. B* **53**, 7376 (1996); *ibid.* **58**, 6800 (1998).
- [14] D.Varsano, S.Moroni, and G.Senatore, *Europhys. Lett.* **53**, 348 (2001).
- [15] S.I. Shevchenko, *Phys. Rev. Lett.* **72**, 3242 (1994).
- [16] S.Conti, G. Vignale and A.H. MacDonald, *Phys. Rev.* **B 57**, 6846 (1998).
- [17] C. Comte and P.Nozieres, *J. Phys.* **43**, 1069 (1982); P.Nozieres and C. Comte, *ibid.* **43**, 1083 (1982).
- [18] We tried a variational gaussian and the form of Ref. 10.
- [19] The electron and hole triangular lattices are chosen in the energetically favored AA stacking.
- [20] F. Rapisarda, PhD Thesis, Università di Trieste (1995).
- [21] For the EP J is constructed using the 2CP pseudopotentials. Depending on coupling the pseudopotentials between paired particles or even all interlayer pseudopotentials may be dropped, to optimize the variational energy.
- [22] D.Ceperley, *Phys. Rev. B* **18**, 3126 (1978).
- [23] The functional forms of Ref. 24, which have proven satisfactory also for the electron bilayer [20], have been used for the normal phases and with minor adaptations (like $E_N = E_\infty + b_2(r_s)/N^\alpha(r_s)$) also for the EP.
- [24] B. Tanatar and D.M. Ceperley, *Phys. Rev.* **B 39**, 5005 (1989).
- [25] G. Senatore, S. Moroni, and D. Varsano, *Solid. St. Comm.* **119** 333 (2001).
- [26] Our energies do not include the phase independent Hartree term $2d/r_s$, accounting for the electric field present if the layers are not separately neutralized.
- [27] We only consider 2DEG studies using Slater-Jastrow trial functions—the same chosen here for the normal phases.
- [28] F. Rapisarda and G. Senatore, *Aust. J. Phys.* **49**, 161 (1996).
- [29] G. Senatore, F.Rapisarda and S. Conti, *Int. Jour. Mod. Phys.* **B 13**, 479 (1999).
- [30] Lerwen Liu, L. Swierkowsky and D.Neilson, *Physica* **B 249**, 594 (1998).
- [31] C.N. Yang, *Rev. Mod. Phys.* **34**, 694 (1962).
- [32] To reduce size effects only the pair in the simulation *box* is displaced, while its periodic copies are held fixed. We have indeed found that this procedure, which is an obvious extension of the one introduced in Ref. 33 for the one-body density matrix, substantially reduces size effects in VMC simulations with $N = 42, 58, 114$.
- [33] W.R Magro and D.M. Ceperley *Phys. Rev. Lett.* **73**, 826 (1994).
- [34] D.M.Ceperley and M.H.Kalos, in *Monte Carlo Methods in Statistical Physics*, K.Binder, ed. (Springer, N.Y., 1979).